Available online at www.sciencedirect.com
ScienceDirect
International Journal of Thermal Sciences 47 (2008) 126–135
International Journal of Thermal Sciences
www.elsevier.com/locate/ijts

Simulation of Ludwig–Soret effect of a water–ethanol mixture in a cavity filled with aluminum oxide powder under high pressure

C.G. Jiang [a], T.J. Jaber [a], H. Bataller [b], M.Z. Saghir [a,*]

[a] *Ryerson University, Department of Mechanical and Industrial Engineering, ON, Canada*
[b] *Laboratoire des Fluides Complexes, Université de Pau, Pau Cedex, France*

Received 28 July 2006; received in revised form 9 January 2007; accepted 9 January 2007

Available online 26 February 2007

Abstract

Thermosolutal convection of a water–ethanol binary mixture, with a 50% mass fraction, at a high pressure of 750 bar, in a three-dimensional horizontal cavity, filled with an aluminum oxide (Al_2O_3) porous medium, is numerically investigated. Such investigation is examined in terms of the compositional separation versus the thermal conductivity and permeability of Al_2O_3 porous medium. The thermal diffusion, or Soret effect, is analyzed globally with a separation ratio and locally with the distributions of ethanol mole fraction on the horizontal and vertical lines in the center of the porous cavity. The Soret coefficient of ethanol at 30 °C was found to vary between −0.00699 and −0.00610 when pressure increases from 1 to 750 bar, leading to a ±13.74% relative variation around the mean value. On the other hand, the Soret coefficient of ethanol at 750 bar will vary from −0.00697 to −0.00534 when the temperature increases from 10 to 50 °C, leading to ±26.48% relative variation around the mean value. The details of the compositional separation at the steady state of thermosolutal convection are also applied to study the characteristics of Soret effect. When the value of permeability is less than 10^4 md, the compositional separation in the cavity is evident. However, when the value of permeability is larger than 10^4 md, the thermosolutal convection creates a mixing of the substances and the separation is diminished. Recommendations are made for the experimental design based on the results of numerical analysis.

Keywords: Soret effect; Porous media; Convection; Thermodynamics; Separation

1. Introduction

In recent years, thermal diffusion, or the Soret effect, has become a subject of extensive scientific research both theoretically and experimentally. As well, as a result of its wide engineering and technological applications in many areas, research on thermal-solutal convection in porous media has gained more and more attention. Such attention has been focused on areas including underground diffusion of nuclear waste, oil reservoir analysis, petroleum extraction, mineral material migration, separation of mixtures.

In 1857, Ludwig [1] reported his discovery of the molecule segregation phenomenon of a mixture under temperature gradient; Soret [2] later conducted a comprehensive and systematic research on this phenomenon, named the Soret effect. Based on the non-equilibrium thermodynamics theory of De Groot [3], many models were proposed to predict the thermal diffusion coefficient as well as the Soret coefficient based on properties of components and properties of mixtures, such as the Haase model [4] and the Firoozabadi model [5]. In other literature, the Firoozabadi model was shown to have a stronger performance in predicting the thermal diffusion coefficient, as well as the Soret coefficient, among available models in both hydrocarbon mixtures [5] and water–alcohol mixtures [6].

Water and ethanol mixtures are typical materials in a wide range of areas, such as oil reservoirs. As a result, water–ethanol binary mixtures have been widely used in thermal diffusion research. As well, many available studies have focused on the measurement of the Soret coefficient of water–ethanol mixtures in a range of temperatures under atmosphere pressure. Van Velden [7] measured the Soret coefficient of water–ethanol mixtures with different compositions at 40 °C, and showed the sign change of Soret coefficient at a certain composition of ethanol

* Corresponding author.
E-mail address: zsaghir@ryerson.ca (M.Z. Saghir).

1290-0729/$ – see front matter
doi:10.1016/j.ijthermalsci.2007.01.019

Nomenclature

C_p	Heat capacity at constant pressure	$J\,kg^{-1}\,K^{-1}$	
D_m	Molecular diffusion coefficient	$m^2\,s^{-1}$	
D_m^*	Molecular diffusion coefficient in porous media	$m^2\,s^{-1}$	
D_T	Thermal diffusion coefficient	$m^2\,s^{-1}\,K^{-1}$	
D_T^*	Thermal diffusion coefficient in porous media	$m^2\,s^{-1}\,K^{-1}$	
D_P	Pressure diffusive coefficient	$m^2\,s^{-1}\,Pa^{-1}$	
D_P^*	Pressure diffusion coefficient in porous media	$m^2\,s^{-1}\,Pa^{-1}$	
J_1	Mass diffusive flux	$kg\,m^{-2}\,s^{-1}$	
$\vec{J}_m$	Molar diffusive flux	$mol\,m^{-2}\,s^{-1}$	
k	Thermal conductivity	$W\,m^{-1}\,K^{-1}$	
L_{ij}	Onsager coefficient		
md	Milli-darcy (0.001 darcy) is a unit of permeability		
P	Pressure	Pa	
q	Separation ratio		
S_T	Soret coefficient	K^{-1}	
T	Temperature	K	
t	Time	s	
u	Velocity component in x-direction	$m\,s^{-1}$	
v	Velocity component in y-direction	$m\,s^{-1}$	
$\vec{V}$	Fluid velocity vector (u, v, w)	$m\,s^{-1}$	
w	Velocity component in z-direction	$m\,s^{-1}$	
x_1	Mole fraction of component 1		
x	Dimension	m	
y	Dimension	m	
z	Dimension	m	

Greek symbols

ϕ	Porosity		
κ	Permeability	m^2	
μ	Dynamic viscosity of the fluid mixture	$kg\,m^{-1}\,s^{-1}$	
ρ	Fluid mixture density	$kg\,m^{-3}$	
ρ_m	Fluid mixture molar density	$kmole\,m^{-3}$	
ω	Mass fraction		

Subscripts

e	effective
f	fluid mixture
m	molar quantities
p	porous media

(13.20% mole fraction). However, his results were two or three times smaller than recently reported results. Tichacek et al. [8] also measured a wide range of ethanol compositions of water–ethanol mixtures at 25 °C and had a stronger agreement with recently reported results. Using a modern laser beam deflection technique, Kolodner et al. [9] measured the Soret coefficient of water–ethanol at a range of ethanol mole fraction from 0.9688 to 20.09% and temperature range from 10 to 40 °C, producing the sign change of Soret coefficient at 14.20% ethanol mole fraction. Koehler and Muller [10] applied Thermal Diffusion Forced Rayleigh Scattering (TDFRS) laser technique to obtain the Soret coefficient of a water–ethanol mixture, and verified one result in Kolodner's report at 25 °C. Zhang et al. [11] used modern laser beam deflection technique and verified the whole range of compositions of water–ethanol mixtures in Kolodner's report at 25 °C. Dutrieux et al. [12] used thermogravitational column (TGC) technique and measured Soret coefficient for two compositions of water–ethanol mixtures at 22.5 °C. They compared their results with other research groups. Wiegand [13] applied TDFRS laser technique to measure a wide range of compositions (from about 5 to 90% ethanol mole fraction) of water–ethanol mixtures at 22 °C, and the sign change in experimental results happened at the mole fraction of ethanol about 13.78%. However, there is no experimental data available for water–ethanol mixtures under a high pressure of 750 bar. The rational for conducting the calculation at a pressure of 750 bar is to mimic in the laboratory a real oil reservoir experiment.

Research on thermal diffusion measured in porous media has also been conducted and reported in various literatures. As a result of the geothermal gradient, the Soret effect naturally exists in places such as in underground crude oil; as well, since porous media can restrain natural convection, it is also applied in thermal gravitational column of experiments. Boutana et al. [14] studied the natural convection in a rectangular porous medium filled with a binary mixture analytically and numerically, and focused on the characteristics of fluid mechanics with given constant Soret coefficient. Alex and Patil [15] investigated the Soret effect on patterns of convection flow in variable gravity fields in a porous medium layer. Both papers used constant Soret coefficients, without regarding to any specified mixture. Costeseque and Platten [16] conducted experiments on the Soret effect in porous media and investigated the details of thermal diffusion process to answer a raised question: "Is the Soret coefficient the same in a free liquid and in a porous medium?" They found that the Soret coefficients are close in their experiments but the thermal diffusion coefficients are not; as a result, a parameter, tortuosity of the porous medium was defined. Later on, Costeseque et al. [17] carefully measured the tortuosity of a $CuSO_4$ porous medium and concluded that the tortuosities for thermal diffusion coefficient and molecular diffusion coefficient are approximately equal. The dispersion phenomena of thermal diffusion in porous media were also analyzed [18].

In this study, the thermal-solutal convection of a water–ethanol binary mixture is investigated numerically. This could provide valuable information for experimental design. The physical model and properties of the mixture and the porous medium are presented in Section 2. Section 3 presents the mathematical equations to describe the mass continuity, velocity, and energy transfer. Lastly, the numerical simulation results are discussed in Section 4, and the conclusion is addressed in Section 5.

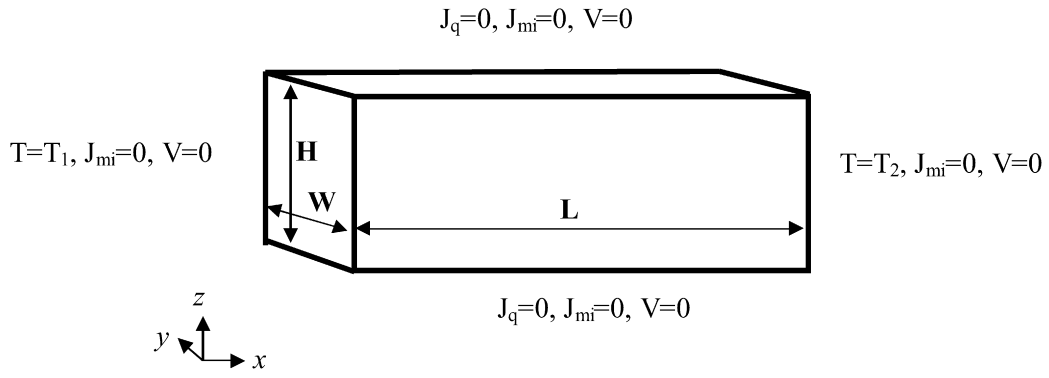

Fig. 1. Schematic diagram of the horizontal porous cavity.

Table 1
Date of Al_2O_3 porous medium and the water–ethanol mixture

Porous cavity length L	32.1 mm
Porous cavity width W	10.0 mm
Porous cavity height H	10.0 mm
Left wall temperature T_1	10 °C
Right wall temperature T_2	50 °C
Pressure at the center of the cavity	750 bar
Al_2O_3 molecular weight	101.961 kg kmol^{-1}
Al_2O_3 density	3983.6 kg m^{-3}
Al_2O_3 heat capacity	786.2745 J kg^{-1} K^{-1}
Al_2O_3 thermal conductivity	43 W mol^{-1} K^{-1}
Al_2O_3 porosity	0.4
Al_2O_3 porous medium permeability	10^{-10}–10^{-8} m^2 (10^5–10^7 md)
Al_2O_3 porous medium tortuosity	1.3
Water–ethanol mixture compositions	50%–50% (mass fraction)
Water–ethanol mixture heat capacity	3328.6 J kg^{-1} K^{-1}
Water–ethanol mixture thermal conductivity	0.39 W m^{-1} K^{-1}

2. Physical model

As shown in Fig. 1, the porous cavity has a horizontal length of 32.1 mm, a width of 10 mm, and a vertical height of 10 mm. The porous material inside the cavity is Al_2O_3 powder, and saturated with a water–ethanol binary mixture. The binary mixture of water–ethanol used in this research is with a 50% mass fraction for both water and ethanol (28.1167 and 71.8833% mole fractions of ethanol and water, respectively). The nominate pressure at the center control volume of the porous cavity is 750 bar. The left wall is maintained at a constant temperature of 10 and the right wall at 50 °C, forming the lateral heating condition. All data for both the mixtures and the porous medium are shown in Table 1.

Due to thermal expansion and the Soret driving separation, the thermosolutal natural convection will be initialized under the gravity field and reach a steady state in a time process.

3. Mathematical formula

In a three-dimensional porous cavity, the mass continuity equation is written as:

$$\frac{\partial \rho_m}{\partial t} + \frac{\partial(\rho_m u)}{\partial x} + \frac{\partial(\rho_m v)}{\partial y} + \frac{\partial(\rho_m w)}{\partial z} = 0 \tag{1}$$

where ρ_m is the molar density of the fluid mixture, and u, v and w are the two horizontal (x and y directions) velocity components and the vertical velocity component, respectively. In a binary mixture, the continuity equation of ethanol component is given as:

$$\frac{\partial(\rho_m x_1)}{\partial t} + \frac{\partial(\rho_m u x_1)}{\partial x} + \frac{\partial(\rho_m v x_1)}{\partial y} + \frac{\partial(\rho_m w x_1)}{\partial z} = -\nabla \cdot \bar{J}_m \tag{2}$$

where $\bar{J}_m$ is the molar flux of the solute ethanol; x_1 is the mole fraction of ethanol, usually named concentration for a binary mixture; and the mole flux can be expressed in three diffusion terms,

$$\bar{J}_m = -\rho_m (D_m^* \nabla x_1 + D_T^* \nabla T + D_P^* \nabla P) \tag{3}$$

where T is the temperature, P is the pressure and D_m^*, D_T^*, and D_P^* are the molecular diffusion, thermal diffusion and pressure diffusion coefficients of ethanol in the Al_2O_3 porous medium, respectively, which are related to molecular diffusion coefficient, thermal diffusion coefficient, and pressure diffusion coefficient in free liquid as,

$$\begin{cases} D_m^* = D_m/\tau_m^2 \\ D_T^* = D_T/\tau_T^2 \\ D_P^* = D_P/\tau_P^2 \end{cases} \tag{4}$$

where D_m, D_T, and D_P are the molecular, thermal, and pressure diffusion coefficients, which are functions of the temperature, pressure, and the compositions of the binary mixture. τ_m, τ_T, and τ_P are tortuosities of molecular diffusion, thermal diffusion, and pressure diffusion coefficients of the porous medium Al_2O_3, respectively. Based on Costeseque's research results, the following assumption is made to be applied in this work for the Al_2O_3 porous medium:

$$\tau_m = \tau_T = \tau_P \equiv \tau \tag{5}$$

D_T, D_m, and D_p can be calculated with the Firoozabadi model [17]. The general formula of Firoozabadi model for a

multi-component mixture are shown below in terms of thermodynamic properties and Onsager coefficients,

$$\begin{cases} D_m(i,j) \\ \quad = \dfrac{R}{\rho_m x_n M_n} \displaystyle\sum_{k=1}^{n-1} L_{ik} \frac{x_j M_j + x_n M_n \delta_{jk}}{M_j} \sum_{l=1}^{n-1} \frac{\partial \ln f_j}{\partial x_l}\bigg|_{X,T,P} \\ D_T(i) = \dfrac{L_{iq}}{\rho_m T^2} \\ D_P(i) \\ \quad = \dfrac{1}{\rho_m T x_n M_n} \displaystyle\sum_{k=1}^{n-1} L_{ik} \left[\sum_{j=1}^{n-1} x_i \bar{V}_j + \frac{x_n M_n}{M_k} \bar{V}_k - \frac{1}{\rho_m} \right] \end{cases} \tag{6}$$

where x_i is the mole fraction of component i, M_i is the molecular weight of component i, $M = \sum_{i=1}^{n} M_i x_i$ is the molecular weight of the mixture, $\bar{V}_i$ is the partial molar volume of component i, f_i is the fugacity of component i, R is the gas constant, L_{ik} and L_{iq} are Onsager coefficients, and δ_{ik} is the delta function ($\delta_{ik} = 1$, if $i = k$ and $\delta_{ik} = 0$, if $i \neq k$).

For binary mixtures, the molecular diffusion coefficient, $D_m(i,j)$, the thermal diffusion coefficient, $D_T(i)$, and the pressure diffusion coefficient, $D_P(i)$, are simplified as D_m, D_T, and D_P, respectively, which are used in the above expressions. The theoretical predictions of diffusion coefficients based on the Firoozabadi model have been compared with experimental data obtained for both hydrocarbon mixtures [18] and water–alcohol mixtures [19]. All thermodynamic parameters are calculated with CPA [20] equation of state in this paper.

In porous media, the porous matrix is assumed to be homogeneous and isotropic. Therefore the Darcy equation is applied and expressed in the following form:

$$\vec{V} = -\frac{\kappa}{\phi\mu}(\nabla P - \rho\vec{g}) \tag{7}$$

where ρ is the mass density of the fluid mixture, $\vec{g}$ is the gravitational acceleration vector, κ, μ, and ϕ are the permeability, the dynamic viscosity, and the porosity, respectively. By substituting the Darcy relation expressed in Eq. (7) into the mass conservation equation expressed in Eq. (1), the pressure can be solved from the obtained differential equation.

The thermal energy conservation equation is expressed as follows:

$$\frac{\partial(\rho C_p)_e T}{\partial t} + \phi u \frac{\partial}{\partial x}\big((\rho C_p)_f T\big) + \phi v \frac{\partial}{\partial y}\big((\rho C_p)_f T\big) + \phi w \frac{\partial}{\partial z}\big((\rho C_p)_f T\big) = k_e \left[\frac{\partial^2 T}{\partial x^2} + \frac{\partial^2 T}{\partial y^2} + \frac{\partial^2 T}{\partial z^2} \right] \tag{8}$$

where $(\rho C_p)_e$ is the effective volumetric heat capacity of the system and k_e is the effective thermal conductivity of the system. These effective physical parameters are related to the fluid properties and the solid matrix properties as follows:

$$(\rho C_p)_e = \phi(\rho C_p)_f + (1-\phi)(\rho C_p)_p \tag{9}$$

$$k_e = \phi k_f + (1-\phi) k_p \tag{10}$$

The boundary conditions are zero mass flux at all rigid walls, zero velocity at all rigid walls, fixed temperatures at left wall (10 °C) and right wall (50 °C), and zero thermal flux at other walls, as shown in Fig. 1.

Above equations are discretized with the second-order center differencing scheme in the space discretization and a semi-implicit first-order scheme for the temporal integration, and solved numerically using the control volume method together with corresponding boundary conditions. The non-linear convection terms are treated with the power-law method. The linear algebraic system of discretized equations is solved at one time step after another, with a bi-conjugated gradient iteration method applied to reach converged solution at each time step. The uniform composition, and linear temperature, and zero velocity are used as initial conditions, the convergence criterion is set for variables of composition, temperature, and pressure. The relative errors between internal iteration calculation and any two successive time steps are calculated with the following formula:

(1) for internal iteration at each time step,

$$\gamma_\theta = \frac{1}{nx \times ny \times nz} \sum_{i=1}^{nx} \sum_{j=1}^{ny} \sum_{l=1}^{nz} \left| \frac{\theta_{ijl}^{k,s+1} - \theta_{ijl}^{k,s}}{\theta_{ijl}^{k,s+1}} \right| \tag{11}$$

(2) for convergence checking between two successive time steps after the convergence of the internal iteration,

$$\gamma_\theta = \frac{1}{nx \times ny \times nz} \sum_{i=1}^{nx} \sum_{j=1}^{ny} \sum_{l=1}^{nz} \left| \frac{\theta_{ijl}^{k,s+1} - \theta_{ijl}^{k-1,s0}}{\theta_{ijl}^{k-1,s0}} \right| \tag{12}$$

where θ represents the composition, temperature, and pressure, respectively, i, j, and l represent control volume indices along x, y, and z directions of the porous cavity; k denotes the time step and s is the indicator of inner iterations, and $s0$ is the indicator of the converged inner iteration at last time step. The values of composition, temperature and pressure are defined in the center of each control volume, but the velocities are defined on the surface of each control volume, or grid cell. Different mesh size is tested and a $31 \times 31 \times 31$ control volume has been adopted.

4. Results and discussion

The accuracy of the Firoozabadi model in predicting the thermal diffusion and the Soret coefficients of a water–ethanol mixture was checked in water–ethanol mixtures with the same composition for different temperature and pressure. Since the experimental data under the high pressure of 750 bar is not available, the Soret coefficients was then predicted. Secondly, the effect of the thermal conductivity of Al_2O_3 porous medium on the thermo-solutal convection was investigated. The permeability effect of Al_2O_3 porous medium was analyzed in terms of central x–z plane compositional distribution pattern, central line compositional distribution, and global separation ratio.

4.1. Soret coefficient and thermal diffusion coefficient

There is no experimental data available for the water–ethanol mixture under 750 bar in the working temperature range to

Table 2
Comparison of Soret coefficient, S_T (10^{-3} K^{-1})

Mass fraction of ethanol (%)	Temperature (K)	Pressure (bar)	Exp. [6,12]	Firoozabadi model	Haase model	Kempers model
90%	37.5	1.0013	−1.85	−1.75	−52.86	−61.59
50%	22.5	1.0013	−5.82	−7.28	−189.6	−241.3

Table 3
Comparison with experimental data of thermal diffusion coefficient

	Ethanol mass frac. (–)	T (°C)	P (bar)	D_m (10^{-10} m^2 s^{-1})	D_T (10^{-12} m^2 s^{-1} K^{-1})	S_T (10^{-3} K^{-1})
Exp. [6]	90%	37.5	1.013	15.30	−2.48	−1.85
F. model				16.68	−2.92	−1.75
Exp. [12]	50%	22.5	1.013	4.20	−2.49	−5.82
F. model				5.74	−4.18	−7.28
Prediction	50%	30.0	750	5.78	−3.53	−6.10

compare with. In previous works, the Firoozabadi model was used to estimate the thermal diffusion coefficient of water–ethanol mixtures [6,19]. Generally, when water content is less then 60% in the mixture, the theoretical prediction of the Firoozabadi model is closer to the experimental data. For the water–ethanol mixtures with a 90 and 50% mass fraction of ethanol at 37.5 and 22.5 °C, respectively, the experiment data at atmospheric pressure [6,12] was used to compare with the predictions of the Firoozabadi model. The thermal diffusion flux equation is given below in the experiment:

$$J_1 = -\rho\left(D_m \nabla\omega_1 + D_T \omega_1(1-\omega_1)\nabla T\right) \tag{13}$$

where J_1 is the thermal diffusion mass flux, ω_1 is the ethanol mass fraction, D_m and D_T are the molecular and thermal diffusion coefficients defined in Eq. (13).

Based on Eq. (13), Soret coefficient is defined as below:

$$S_T = \frac{D_T}{D_m} \tag{14}$$

Note that the definition of coefficients D_m and D_T in Eqs. (13) and (14) are given in mass frame with mass fraction, different from those given in Eqs. (3), (4), and (6), which are defined in molar frame. The transformation for comparison was introduced in previous work [19] and applied here.

Experimental data of two water–ethanol mixtures with different compositions at atmosphere pressure is used to compare with the theoretical predictions of different models: the Firoozabadi model; the Haase model; and the Kempers model [21]. The comparison results are given in Table 2.

For a 90% mass fraction of ethanol, the theoretical prediction of the Firoozabadi model is very close to experiment data. However, both the Haase model and the Kempers model give a very larger magnitude of about thirty times away. For a 50% mass fraction of ethanol, the theoretical prediction of the Firoozabadi model is with 25% relative error, and both the Haase and the Kempers model provide a value of about thirty times higher. In both cases, the Firoozabadi model gives a stronger prediction in terms of comparison with experimental data and will be used in our study.

The main reason for the difference in results between the experiment and the theoretical prediction is due to the effect of hydrogen bonding, which is not considered in this paper.

However Shu et al. [22] using PCSAFT equation of state managed to resolve this discrepancy and recently obtained an excellent agreement with the experimental data available in the literature. For our calculation using CPA equation of state our results are close to Shu et al. [22] results for our conditions.

The variations of the Soret coefficient and the thermal diffusion coefficient of ethanol in the water–ethanol mixture for the pressure range from 1 bar to 750 bar are shown in Fig. 2. The magnitudes of both the Soret coefficient and the thermal diffusion coefficient decrease when the pressure increases, but the variation is not significant with relative errors ±13.74 and ±9.13%, respectively, referred to the mean value of the entire pressure range.

The variations between the Soret coefficient and the thermal diffusion coefficient of ethanol in the water–ethanol mixture at 750 bar for a temperature range of 10 to 50 °C are also calculated and shown in Fig. 3. Both the Soret coefficient and the thermal diffusion coefficient vary approximately linearly in the temperature range of 10 to 50 °C, the relative error of thermal diffusion coefficient is ±10.32% referred to the mean value of the entire temperature range, but the relative error of Soret coefficient is ±26.48%.

The calculated values of molecular and thermal diffusion coefficients, as well as Soret coefficient at 750 bar and 30 °C are summarized in Table 3.

Considering the 25% relative error of the Soret coefficient at atmosphere pressure and the variation of the Soret coefficient versus pressure and temperature, the accuracy of the theoretical prediction of the Firoozabadi model could be quantitatively approximated, and qualitatively analyzed. The numerical simulation of 50%–50% water–ethanol mixture at a pressure of 750 bar in the temperature range of 10 to 50 °C inside a 32.1 mm × 10 mm × 10 mm cavity filled with an Al_2O_3 porous medium is conducted to study the characteristics of the thermosolutal convection on this base.

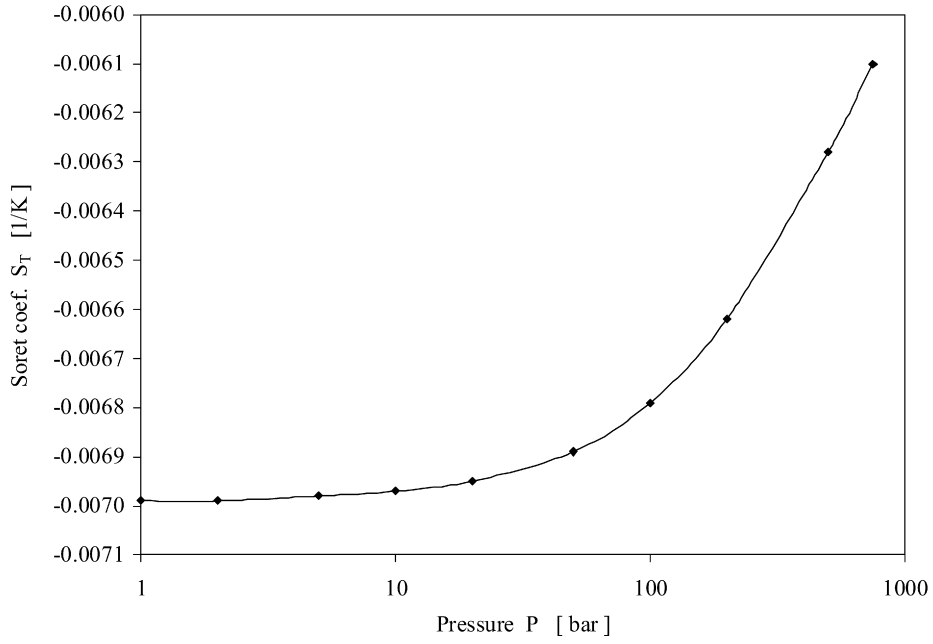

(a) Soret coefficient vs pressure

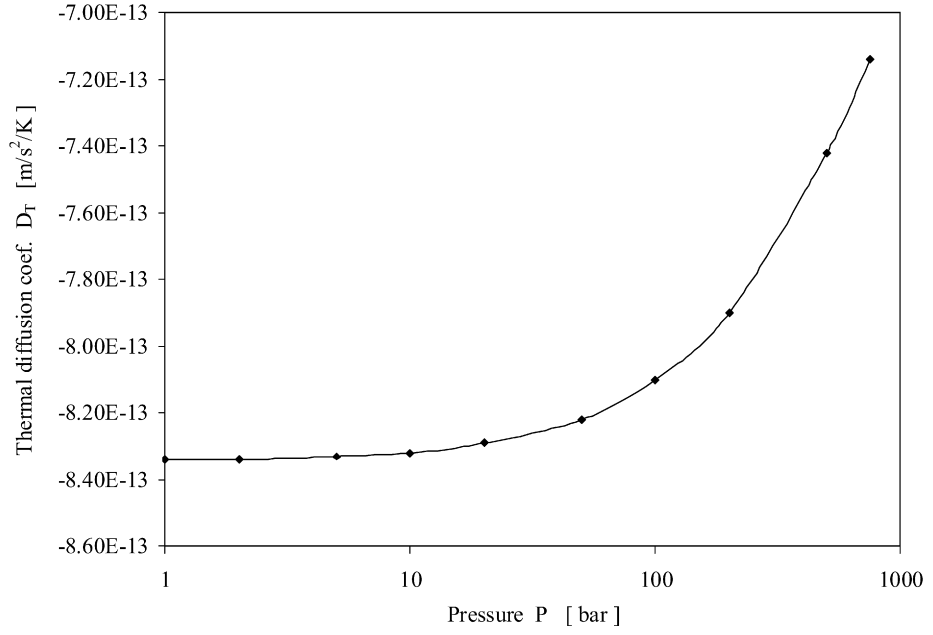

(b) Thermal diffusion coefficient vs pressure

Fig. 2. Soret coefficient and thermal diffusion coefficient as function of pressure at 30 °C.

4.2. Al_2O_3 thermal conductivity effect

Al_2O_3 is crystal, and consists of different structures. The value of its thermal conductivity varies from 43.0 to 6000.0 $W\,m^{-1}\,K^{-1}$, depending on its structure. In order to investigate the thermal conductivity effect on thermo-solutal convection of the water–ethanol mixture in the Al_2O_3 porous medium, the three-dimensional (3D) simulation has been run with these two thermal conductivities for a wide range of permeability. The permeability range applied in this investigation is from 50 md (1 md = 10^{-3} darcy = 0.987×10^{-15} m^2) to 10^7 md, covering the whole interested range in this research. It was observed that both the maximum mole fraction and separation ratio of ethanol, defined in the following equation, in the porous cavity at steady states were identical in the entire range of permeability for different thermal conductivities, 43 and 6000 $W\,m^{-1}\,K^{-1}$.

$$q = \frac{c_{max}/(1-c_{max})}{c_{min}/(1-c_{min})} \tag{15}$$

where c_{max} and c_{min} are the maximum and minimum ethanol mole fractions in the whole porous cavity, respectively.

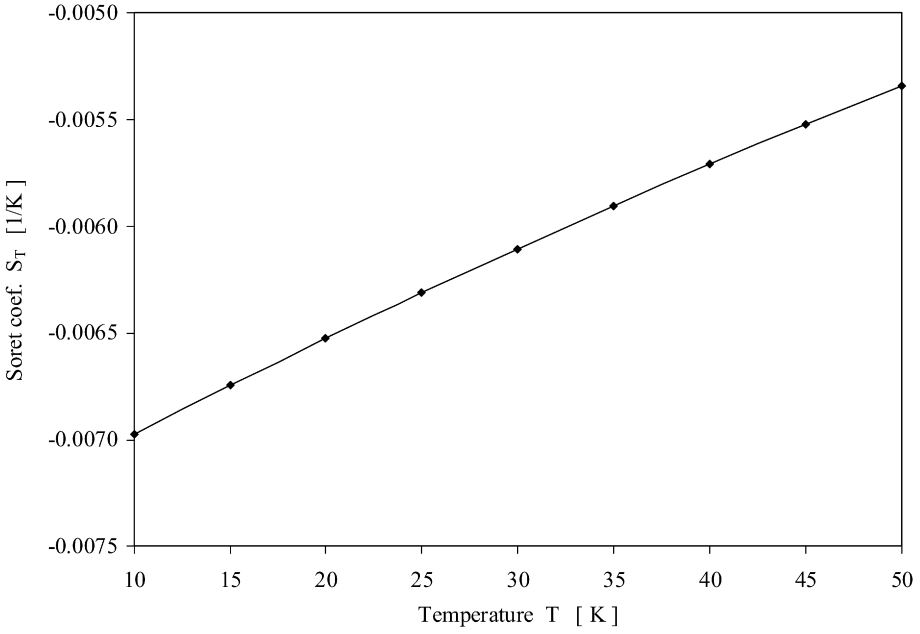

(a) Soret coefficient vs temperature

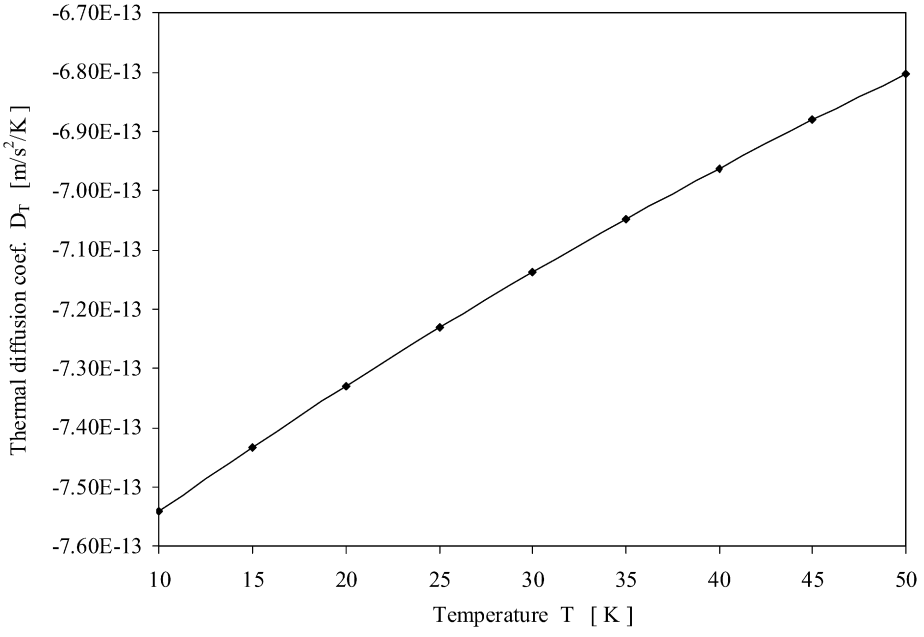

(b) Thermal diffusion coefficient vs temperature

Fig. 3. Soret coefficient and thermal diffusion coefficient as function of the temperature at 750 bar.

The maximum magnitude of q and c_{max} differences was of the order of 10^{-5}, from 10^{-9} order (the 9th digit) for permeability of 50 md to 10^{-5} order (the 5th digit) for permeability of 10^7 md. As the permeability increases, the difference increases. However, the difference is negligible, not significant at all, especially to experimental measurement with available techniques.

Therefore, the thermosolutal convection of the water–ethanol mixture in Al_2O_3 porous cavity is not sensitive to the thermal conductivity of Al_2O_3 porous medium in the interested permeability range of 50 to 10^7 md. The thermal conductivity of 43 W m^{-1} K^{-1} is then adopted in this work.

4.3. Permeability effect

The separation at 10^5 md is identifiable, but at 10^7 md, convective mixing will be dominant over the Soret effect. The values of the separation ratio are 1.0089 and 1.0001, respectively. The two values are so close to 1.0, too small for experimental measurement. As a result of these nonencouraging results, the entire permeability range from 1 to 10^7 md was investigated; the composition distributions at the central x–z plane for cases of 10^2, 10^4, 10^5, and 10^7 md are shown in Fig. 4, and the separation ratio over the entire permeability range is shown in Fig. 5.

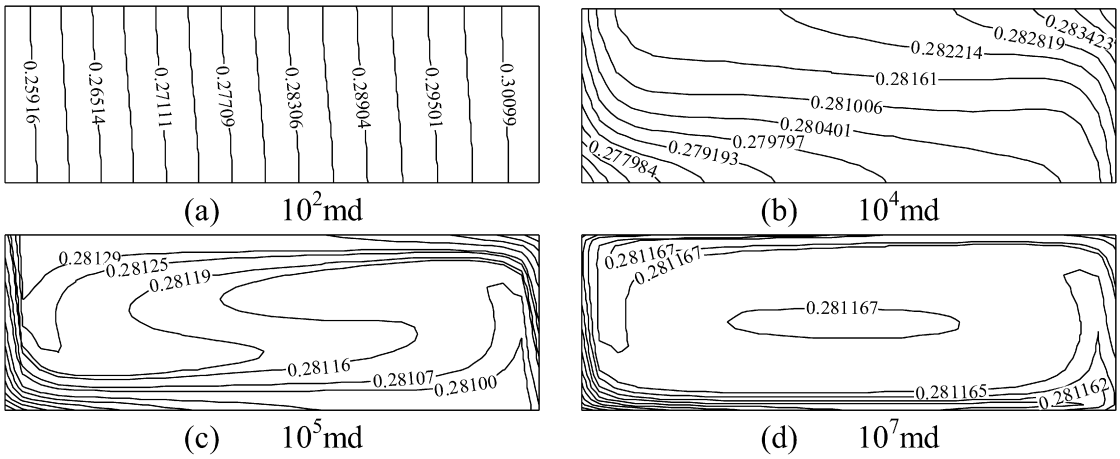

Fig. 4. Ethanol mole fraction distributions in the central x–z plane.

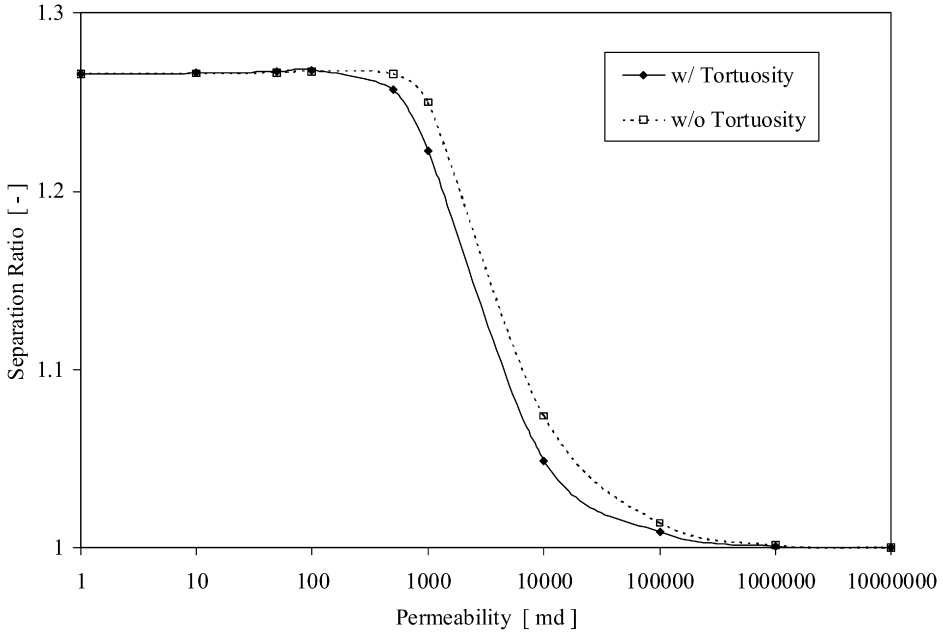

Fig. 5. Permeability and tortuosity effect on the separation in porous media.

For permeability of 10^2 and 10^4 md, the separation ratio is evident with a clear distribution pattern with high concentration of ethanol appearing at the hot wall towards the top corner as shown in Fig. 4. The values of the separation ratio are 1.2681 and 1.0491, respectively. As the permeability increases beyond 10 000 md, convective mixing is more evident and separation ratio is reduced to one; Fig. 4 shows a uniform distribution of ethanol in the mixture.

In Fig. 5, it can be observed that convection has little positive effect on compositional separation process with permeability less than 10^2 md and significantly negative effect on compositional separation when permeability larger than 10^2 md. This may be due to the large value of thermal conductivity of Al_2O_3 medium in one part and the small aspect ratio, ~0.3 of the cavity.

The tortuosity of the Al_2O_3 medium is 1.3, and the separation ratio without tortuosity considered is also shown in Fig. 5. It is noticeable that with and without tortuosity, for both the thermal diffusion dominant part and the convection dominant part, the two curves merge together. However, at the middle range of permeability, approximately from 10^2 to 10^5 md, the separation ratio with tortuosity taken into consideration is smaller than the values without tortuosity. The maximum difference is found to be 2.37%. This is reasonable, in light of the smaller thermal diffusion coefficients for the tortuosity considered cases.

The separation ratio shows the maximum separation in the entire porous cavity, but lack of detail information. The ethanol mole fraction distributions in the horizontal x and vertical z lines in the center of the porous cavity present more information about the separation situation at the steady state of the thermosolutal convection.

The horizontal x direction distributions of ethanol mole fraction in the center of the porous cavity at different values of permeability are shown in Fig. 6. The magnitude of the separation consistently declines as the value of permeability increases.

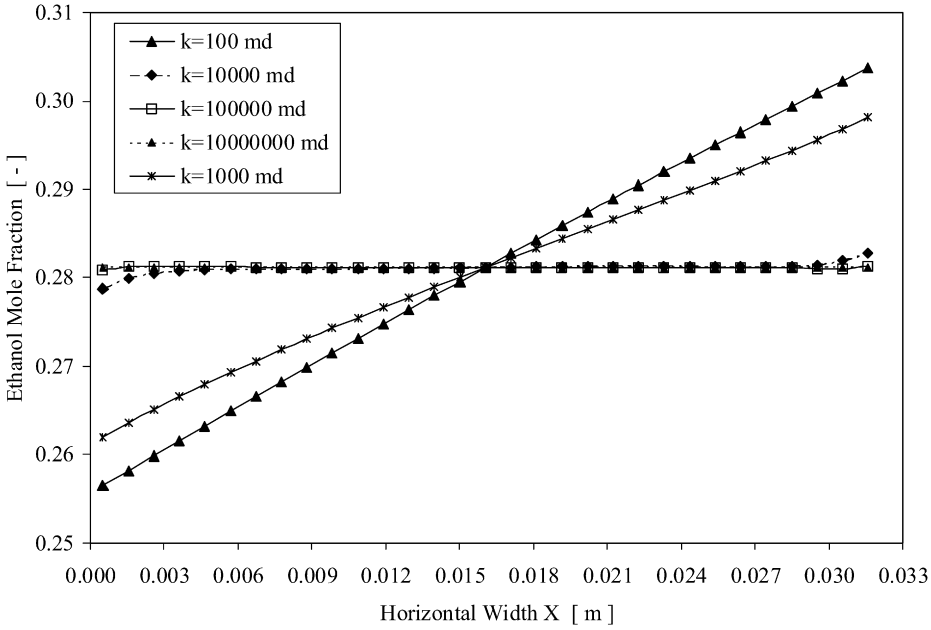

Fig. 6. Ethanol mole fraction distributions along the central x horizontal line.

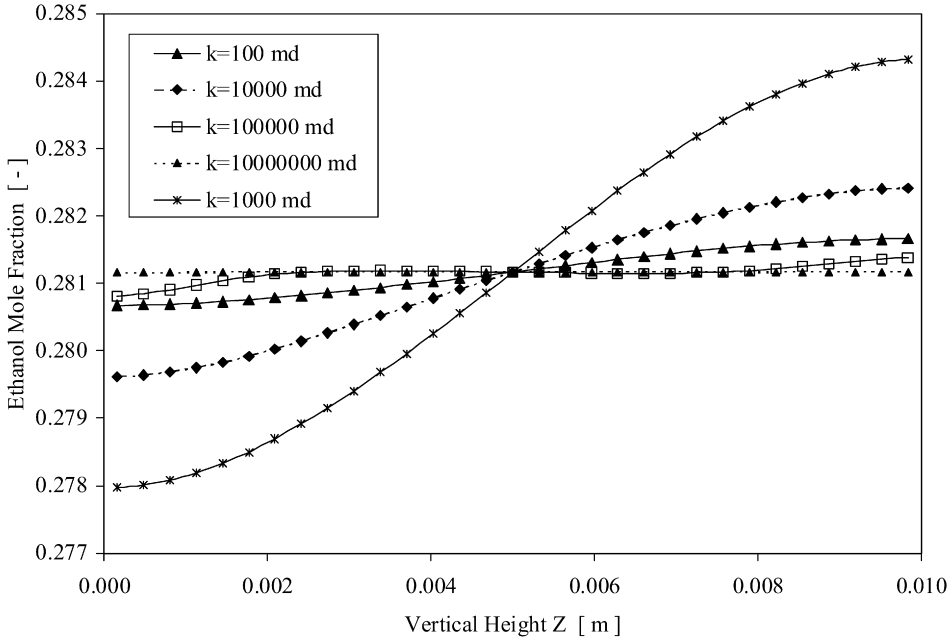

Fig. 7. Ethanol mole fraction distributions along the central z vertical line.

It is important to notice that the horizontal separation at 10^4 md permeability is small, compared to the separation at 10^3 and 10^2 md, and the horizontal separation at 10^5 and 10^7 md are indistinguishable, since the convection causes the mixing of compositions.

In Fig. 7, the vertical distributions of ethanol mole fraction in the center of the porous cavity at different values of permeability are presented. The vertical separation from 10^2 to 10^3 md increases as permeability increases; from 10^3 to 10^7 md, the vertical separation declines continuously as the permeability increases.

5. Conclusion

Both the Soret coefficient and the thermal diffusion coefficient are unknown and subject to experimental exploration in the thermosolutal convection of a water–ethanol mixture with 50% mass fraction each in an Al_2O_3 porous medium cavity at a pressure of 750 bar in the temperature range of 10 to 50 °C. Numerical investigation can provide qualitative and useful information for the experiment design. The accuracy of the Firoozabadi model with 25% relative error in predicting the Soret coefficient is examined with comparison to the Hasse

model and the Kempers model for two water–ethanol mixtures at atmosphere pressure, based on available experimental data. The 13.74 and 26.48% variations of the Soret coefficient in the pressure range of 1 bar to 750 bar at temperature 30 °C and in the temperature range of 10 to 50 °C at pressure 750 bar, respectively, are also analyzed. The investigation of thermosolutal convection shows that the thermal conductivity of Al_2O_3 has no significant effect on the compositional separation process, but the permeability of Al_2O_3 porous medium has definitely dominant effect on the compositional separation at the steady state of the thermosolutal convection. When the value of permeability is less than 10^4 md, the compositional separation in the cavity is evident with certain distribution pattern. However, when the value of permeability is larger than 10^4 md, the thermosolutal convection creates mixing in the mixture and the separation is diminished. Instead of a permeability range from 10^5 to 10^7 md, the permeability range of 10^2 to 10^4 md is recommended, and the porosity of 0.4 should be adjusted to 0.2 correspondingly in experiment applications. Finally in order to observe the Soret effect in the experiment the following findings must be implemented:

(1) the permeability of Al_2O_3 porous medium should be in the range of 10^2 and 10^4 md, instead of 10^5 and 10^7 md;
(2) the porosity of the porous medium, 0.4, may need to be reduced to 0.2, in accordance with the decrease of the permeability;
(3) the aspect ratio, 0.3, of the horizontal cavity gives the separation ratio of thermal diffusion limited by thermal diffusion itself, no gain from the contribution of thermosolutal convection flow.

Acknowledgements

The authors acknowledge the full support of Natural Sciences and Engineering Council (NSERC) for funding this project.

References

[1] C. Ludwig, Sitzungsber. K. Preuss, Akad. Wiss. 20 (1856) 539.
[2] C. Soret, Influence de la temperature sur la distribution des sels dans leurs solutions, Compte-Rendu de l'Academie des Sciences, Paris 91 (1880) 289.
[3] S.R. De Groot, P. Mazur, Non-Equilibrium Thermodynamics, Dover Publication Inc., New York, 1984.
[4] R. Haase, Thermodynamics of Irreversible Processes, Addison–Wesley Publishing Company, Reading, MA, 1969.
[5] K. Shukla, K.A. Firoozabadi, A new model of thermal diffusion coefficients in binary hydrocarbon mixtures, Industrial Engrg. Chem. Res. 37 (1998) 3331.
[6] M.Z. Saghir, C.G. Jiang, S.O. Derawi, E.H. Stenby, M. Kawaji, Theoretical and experimental comparison of the Soret coefficient for water–methanal and water–ethanol binary mixtures, Eur. Phys. J. E 15 (2004) 241.
[7] P.F. Van Velden, Etude sur la diffusion thermique dans des melanges liquides alcool–eau au moyen de la methode thermogravitationanelle de separation, Physica XII 2–3 (1946) 151.
[8] L.J. Tichacek, W.S. Kmak, H.G. Drickamer, Thermal diffusion in liquids: the effect of non-ideality and association, J. Phys. Chem. 60 (1956) 660.
[9] P. Kolodner, H. Williams, C. Moe, Optical measurement of the Soret coefficient of ethanol/water solution, J. Chem. Phys. 88 (10) (1988) 6512.
[10] W. Kohler, B. Muller, Soret and mass diffusion coefficients of toluene/*n*-hexane mixtures, J. Chem. Phys. 103 (1995) 4367.
[11] K.J. Zhang, M.E. Briggs, R.W. Gammon, J.V. Sengers, Optical measurement of the Soret coefficient and the diffusion coefficient of liquid mixtures, J. Chem. Phys. 104 (17) (1996) 6881.
[12] J.F. Dutrieux, J.K. Platten, G. Chavepeyer, M.M. Bou-Ali, On the measurement of positive Soret coefficients, J. Phys. Chem. B 106 (2002) 6104.
[13] S. Wiegand, Sign change of Soret coefficient of polyethylene oxide in water/ethanol mixtures observed by Thermal Diffusion Forced Rayleigh Scattering, J. Chem. Phys. 121 (8) (2004) 3874.
[14] N. Boutana, A. Bahloul, P. Vasseur, F. Joly, Soret-driven and double diffusive natural convection in a vertical porous cavity, J. Porous Media 7 (1) (2004) 41.
[15] S.M. Alex, P.R. Patil, Effect of variable gravity field on Soret driven thermosolutal convection in a porous medium, Int. Commun. Heat Mass Transfer 28 (4) (2001) 509.
[16] P. Costeseque, J.K. Platten, The Soret coefficient in porous media, in: Proceedings of APM2002, 1st International Conference on Applications of Porous Media, Jerba, Tunisia, June 2–8, 2002.
[17] P. Costeseque, T. Pollak, J.K. Platten, M. Marcoux, Transient-state method for coupled evaluation of Soret and Fick coefficients, and related tortuosity factors, using free and porous packed thermodiffusion cells: application to $CuSO_4$ aqueous solution (0.25 M), Eur. Phys. J. E 15 (2004) 1.
[18] D. Fargue, Ph. Jamet, P. Costeseque, Dispersion phenomena in thermal diffusion and modeling of thermogravitational experiments in porous media, Transport in Porous Media 30 (1998) 323.
[19] C.G. Jiang, M.Z. Saghir, M. Kawaji, The accuracy of the theoretical calculation of the Soret coefficient for water–ethanol mixtures with comparison to experimental data, J. Non-Equilibrium Thermodyn. 30 (2005) 337.
[20] M.L. Michelsen, E.M. Hendriks, Physical properties from association models, Fluid Phase Equilibria 180 (2001) 165.
[21] L.J.T.M. Kempers, A thermodynamic theory of the Soret effect in a multicomponent liquid, J. Chem. Phys. 90 (1989) 6541.
[22] S. Pan, Y. Yan, C.G. Jiang, M. Khawaji, M. Kawaji, M.Z. Saghir, Theoretical prediction of thermal diffusion coefficients for ternary hydrocarbon mixtures, in: Proceedings of 7th International Meeting on Thermodiffusion (IMT7), Donostia–San Sebastian, Spain, May 29 – June 2, 2006.